P. KWOLEK*, T. TOKARSKI*, T. ŁOKCIK*, K. SZACIŁOWSKI *,**

NOVEL, MICROWAVE ASSISTED ROUTE OF SYNTHESIS OF BINARY OXIDE SEMICONDUCTING PHASES – PbMoO$_4$ AND PbWO$_4$

NOWA METODA SYNTEZY BINARNYCH FAZ TLENKOWYCH O CHARAKTERZE PÓŁPRZEWODNIKOWYM W POLU MIKROFALOWYM – PbMoO$_4$ I PbWO$_4$

Highly crystalline powders of lead molybdate and tungstate were synthesized by a microwave assisted hydrothermal process in a microwave heated high pressure autoclave. Application of this novel and environmentally friendly technique in the synthesis of these compounds has never been reported before. The influence of a time of synthesis on a crystal structure, morphology and a value of a band gap for both PbMoO$_4$ and PbWO$_4$ was examined. The value of the band gap was determined using diffuse reflectance spectroscopy. For lead molybdate the medium value of the band gap equals to *ca.* 3.2 eV whereas for lead tungstate it oscillates around 4 eV and does not depend on the duration time of the synthesis.

Keywords: lead molybdate, lead tungstate, semiconductor, band gap, microwave assisted synthesis

Krystaliczne proszki molibdenianu ołowiu i wolframianu ołowiu otrzymano metodą hydrotermalną w polu mikrofalowym za pomocą wysokociśnieniowego autoklawu mikrofalowego. Metodę tą można uznać za przyjazną dla środowiska, jak dotąd nie odnotowano jej zastosowania do syntezy wymienionych związków ołowiu. Zbadano wpływ czasu trwania procesu na strukturę krystaliczną, morfologię i szerokość przerwy energetycznej proszków PbWO$_4$ i PbMoO$_4$. Szerokość pasma wzbronionego wyznaczono za pomocą spektroskopii refleksyjnej. Dla molibdenianu ołowiu otrzymane wartości oscylują wokół 3.2 eV, natomiast dla wolframianu ołowiu przerwa energetyczna jest szersza i wynosi ok. 4 eV. Szerokość pasma wzbronionego w obu przypadkach nie zależy od czasu syntezy.

1. Introduction

Metal oxides as well as more complex materials (*e.g.* binary and ternary oxide phases) attract more and more attention due to their semiconducting properties. They are readily studied mainly towards photocatalytic, photovoltaic or optoelectronic applications. Besides the type of a conductivity (*i.e. n* or *p*) one of the most important feature characterizing semiconducting material is the value of the band gap. The character of an intraband transition (*i.e.* direct or indirect) as well as charge carriers mobilities are also of a great importance.

Lead molybdate PbMoO$_4$ is a highly ionic compound with a small contribution of a covalent bonding. It crystallizes in the scheelite-type tetragonal system ($I4_1$/a space group). The crystal consists of MoO$_4$ tetrahedra which are connected to each other via Pb^{2+} ions [1]. DFT calculations indicated, that PbMoO$_4$ is the indirect band gap semiconductor and the value of the gap equals to 2.59 eV [1], however it is well known, that this method leads to underestimated results. The experimental values are in the range between 3.1 and 3.2 eV [2, 3].

The valence band of lead molybdate in the vicinity of the band edge is composed mainly of oxygen 2p orbitals, whereas molybdenum 4d and 5d orbitals occur deeper into the valence band (below *ca.* 3.5 eV from the band edge) and dominates the conduction band close to the conduction band edge. Contribution of the 5s and 5p Mo orbitals to the both bands is negligible. Lead 6s orbitals in turn contribute to the valence band slightly below its edge whereas the 6p states to the conduction band [1].

Lead tungstate PbWO$_4$ similarly to lead molybdate is the highly ionic compound. At the ambient temperature it adopts two types of the crystal structures, namely the tetragonal sheelite-type (the mineral is called stolzite), space group $I4_1$/a [4], composed of the WO$_4$ tetrahedra linked to each other via Pb^{2+} ions and a monoclinic (the mineral is called raspite), space group P 2/n composed of WO$_6$ octahedra. Raspite transforms irreversibly into the stolzite at the elevated temperature (around 400°C) [5]. PbWO$_4$ similarly to PbMoO$_4$ is the indirect band gap semiconductor as it was indicated by DFT calculations. Again the calculated value of the gap is underestimated and equals to 2.96 eV [1].

The electronic structure of lead tungstate is analogous to the electronic structure of lead molybdate. The valence band near the band edge is composed mainly of the oxygen 2p and

*   AGH UNIVERSITY OF SCIENCE AND TECHNOLOGY, FACULTY OF NON-FERROUS METALS, 30-059 KRAKÓW, AL. MICKIEWICZA 30, POLAND

**   JAGIELLONIAN UNIVERSITY, FACULTY OF CHEMISTRY, 30-060 KRAKÓW, 30 INGARDENA STR., POLAND

lead $6s$ orbitals, with some contribution from the tungsten $4d$ and $5d$ orbitals deeper into the band. The conduction band in turn is composed mainly of the W $4d$ and $5d$ orbitals with some contribution from the Pb $6p$ states [1, 6].

Both $PbMoO_4$ and $PbWO_4$ are promising materials for a construction of low temperature scintillators [7]. Recently, the photocatalytic properties of these compounds were studied towards their application in the photoelectrolysis of water and the mineralization of organic pollutants in wastewater [2, 3, 8, 9]. Lead tungstate was also examined towards the application in an electromagnetic calorimetry in the particle physics [10] and is currently used as the scintillator in detectors at the Large Hadron Collider in CERN [11]. $PbMoO_4$ in turn is extensively employed in acousto-optic devices due to its high acousto-optic figure of merit and a low optical loss below 1 GHz [12].

Monocrystals of both $PbMoO_4$ and $PbWO_4$ for the opto-electronics and scintillators are grown by the Bridgman and Czochralski methods [8, 10, 13-16]. On the other hand, the synthesis of both compounds from aqueous solutions becomes more and more popular because of low costs and easy modification of the obtained material. The simplest technique is a precipitation of $PbMoO_4$ or $PbWO_4$ from the solution containing soluble salts of lead and molybdate/tungstate ions. The morphology of lead molybdate obtained with this technique strongly depends on the Pb^{2+}/MoO_4^{2-} ratio [17]. On this method are based another synthetic techniques such as hydrothermal [3, 18], sonochemical [19, 20] or microwave assisted under atmospheric pressure [21]. The CMS technique (composite molten salt) where the reaction was performed in the mixture of molten $LiNO_3$ and KNO_3 was also employed in order to obtain $PbMoO_4$ [2]. Application of these synthetic techniques often leads to obtaining the product in the form of nanoparticles or nanorods [18, 19, 21].

Application of the microwave radiation for a chemical synthesis has numerous advantages, namely the microwave dielectric heating causes the acceleration of the reaction rate in comparison with "classical" heating techniques (*i.e.* oil or sand baths, heating jackets and so on). Moreover, application of the microwave heating in a pressurized system enables conducting the synthetic process above the boiling point of the solvent under ambient pressure. The electromagnetic waves may heat only the solvent and reactants, not the reaction vessel itself. It facilitates avoiding a high temperature gradient in the reaction mixture and ensures more uniform increase of the temperature [22, 23]. Amongst these advantages, shortening the duration of the synthesis is the main benefit. The reaction rate constant k can be described as follows (Eq. 1):

$$k = A \times e^{-\Delta E/RT} \qquad (1)$$

where A is the pre-exponential factor which depends on the frequency of vibrations of the molecules at a reaction interface, ΔE is the activation energy, R is the gas constant and T is the absolute temperature. In the case of dielectric heating, the reaction may be accelerated by the increase of the pre-exponential factor due to the enhanced vibrations of the molecules. However, some authors indicated also the possibility of decreasing the activation energy [24, 25].

The microwave dielectric heating is realized via two mechanisms: a dipolar polarization and a heat conduction. The former is concerned with rotations of the dipolar molecules (*e.g.* water) caused by an alternating electric field of the radiation. The heating is realized via the molecular friction and collisions between the rotating molecules that try to align with the oscillating electric field. The conduction mechanism in turn is caused by ions in solution moving accordingly to the direction of the electric field. Kinetic energy of these ions is efficiently converted to the heat due to collisions. In the case of the synthesis of ternary oxide phases this mechanism seems to be the most important as it facilitates the reaction of ionic precursors. To sum up, in order to perform the microwave heating, a polar solvent and/or ions must be employed. The more polar solvent (*i.e.* the higher dielectric constant), the more efficient microwave heating [22].

However, besides the dielectric properties, the efficiency with which the absorbed energy is converted into heat plays a key role. It is also worth to note, that the dielectric constant strongly depends on the temperature and decreases with the increasing temperature. Therefore, water at the elevated temperature may behave similarly to non-polar solvents. Besides the physicochemical properties of the reagents and a solvent, both a volume and a geometry of the reaction vessel are very important [22].

The aim of this work was to develop a novel, "green" (*i.e.* energy efficient and organic solvent-free) technique of synthesis of lead molybdate and tungstate and to determine the influence of the duration time of the synthesis on the morphology, crystal and energetic structures of the samples.

2. Experimental

The synthesis was performed by a microwave assisted hydrothermal route using a microwave heated high pressure autoclave Magnum II (Ertec, Poland). Lead acetate $(PbCH_3COO).3H_2O$ was applied as a source of lead ions, whereas as precursors for molybdate and tungstate ions were employed sodium molybdate $(Na_2MoO_4.2H_2O)$ and ammonium metatungstate $((NH_4)_6H_2W_{12}O_{40})$ respectively. The reagents were dissolved in deionized water. To prevent the hydrolysis of lead acetate, it was dissolved in water acidified with 1 cm^3 of concentrated acetic acid. All reagents were of analytical grade and were applied without any purification. The reaction mixtures (*i.e.* the mixtures of precursors of lead and molybdate or tungstate ions) were placed in a Teflon vessel and tightly sealed in the autoclave. In order to ensure the reproducible conditions of the synthesis, the total volume for each experiment was the same and equal to 40 cm^3. The reaction mixtures were heated by the microwave radiation and kept at 513 K, the pressure was in the range between 32 and 35 bar. For both $PbMoO_4$ and $PbWO_4$ the influence of the duration time on the product was examined and 3 samples were prepared: after 1, 2 and 4 hours. After completion of the synthesis, the products in the form of fine, white powders were carefully rinsed with deionized water, centrifuged and dried in air. All the parameters of the synthesis are summarized in the TABLE 1.

TABLE 1

Table 1 Parameters of the synthesis for PbMoO$_4$ (samples 1.1 – 1.3) and PbWO$_4$ (samples 2.1 – 2.3)

Sample number	Amount of (PbCH$_3$COO).3H$_2$O	Amount of Na$_2$MoO$_4$.2H$_2$O (samples 1.1-1.3) or (NH$_4$)$_6$H$_2$W$_{12}$O$_{40}$ (samples 2.1-2.3)	Time of the synthesis	Total volume	Temperature	Pressure
	g	g	h	cm^3	K	bar
1.1	1.0335	0.6593	1			
1.2	1.0348	0.6595	2			
1.3	1.0338	0.6601	4	40	513	32 - 35
2.1	0.8336	0.7050	1			
2.2	0.8340	0.7052	2			
2.3	0.8337	0.7048	4			

The crystal structure and a phase composition was determined by an X – ray diffraction (XRD) technique using the Rigaku Miniflex II diffractometer with Cu Kα radiation (λ = 0.15406 nm). The morphology of the samples was examined by the Hitachi SU-70 scanning electron microscope (SEM). In order to characterize the morphology of the obtained powders, the vacuum dried specimens were deposited onto the conductive carbon tape. Low accelerating voltage was used due to a charging effect on the poorly conducting specimens.

In order to determine the value of the band gap diffuse reflectance spectra were recorded on the Lambda 950 spectrophotometer (Perkin Elmer, USA) equipped with 150 mm integration sphere. The samples were dispersed in spectrally pure BaSO$_4$ in the 1:50 weight ratio. The pressed BaSO$_4$ pellet was employed as a 100% reflectivity reference.

3. Results and discussion

When the solutions containing lead and molybdate or tungstate ions are mixed together, the simple precipitation process is observed and the product is formed as follows (Eq. 2):

$$Pb^{2+} + MoO_4^{2-} =\downarrow PbMoO_4 \qquad (2)$$

In the case of PbWO$_4$ the equation will be more complicated due to the more complex stoichiometry of the precursor of tungstate ion. The thermodynamic condition which must be fulfilled to ensure the negative value of the ΔG of such reaction is to exceed the solubility products of PbMoO$_4$ and PbWO$_4$ respectively. For lead molybdate the solubility product equals to 1.2×10^{-13} whereas for lead tungstate it is higher and equals to 8.4×10^{-11} [26]. Such a simple precipitation technique leads to obtaining partially amorphous, poorly crystalline phases, whereas the heat treatment step after the precipitation significantly improves the crystallinity of the powdery material. Adopted synthetic technique should be regarded as an environmentally friendly ("green") technique since no organic solvents are employed and no volatile products of the reaction are emitted. Moreover, the dielectric inereasing temperature by the microwave radiation is the energy efficient way of heating of the reaction mixture. The heating is realized mainly via the conduction mechanism due to the presence of ionic precursors in reaction mixture.

In the Fig. 1 there are presented the X-ray diffraction patterns for the PbMoO$_4$ samples after 1, 2 and 4 hours of the synthesis respectively. They confirm, that the microwave assisted route of synthesis enabled obtaining phase pure, highly crystalline tetragonal structure lead molybdate (ICDD PDF 2010, space group $I4_1$/a). There are no obvious impurities in the sample. In the Fig. 2 in turn there are presented the diffraction patterns for the PbWO$_4$ samples. They confirm the tetragonal structure of the product (ICDD PDF 2010, space group $I4_1$/a). After 1 and 4 hours of the synthesis exclusively tetragonal structure of the sample was obtained, whereas after two hours there is a peak from an impurity indicated by an asterisk. This impurity may originate from a contamination in the synthetic step.
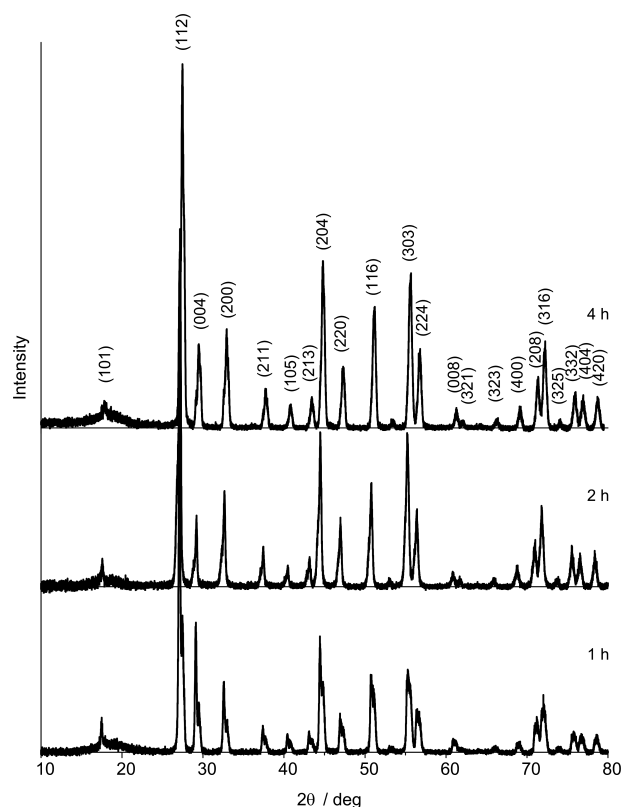

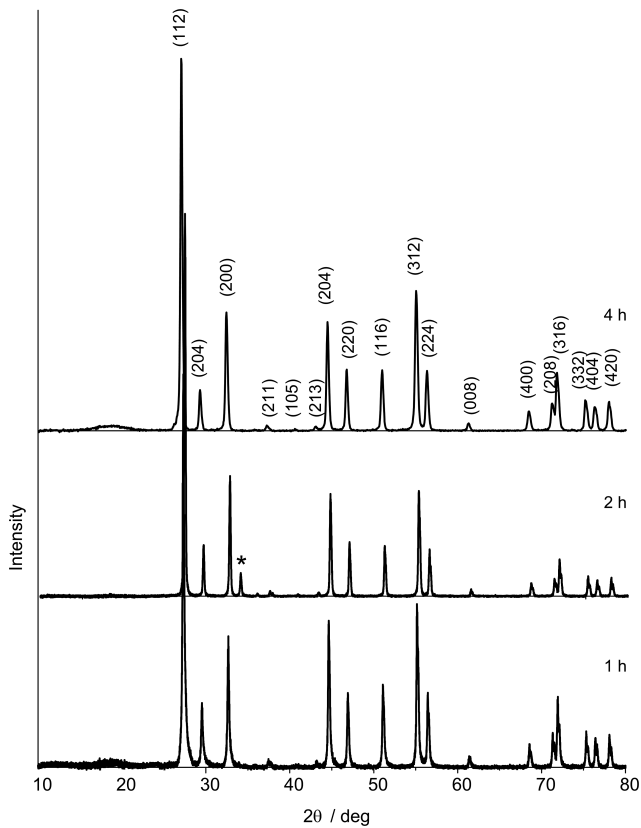Fig. 1. The X-ray diffraction patterns for the PbMoO$_4$ samples after 1, 2 and 4 hours of synthesis

Fig. 2. The X-ray diffraction patterns for the PbWO$_4$ samples after 1, 2 and 4 hours of synthesis

Fig. 3. The SEM images of the PbMoO$_4$ samples (left handside) and PbWO$_4$ (right handside)

The morphology of the obtained powders is presented in the Fig. 3. PbMoO$_4$ particles are equiaxed with well developed crystal faces. Major amount of the particles are in the size between 1 and 2 μm but also the particles around 0.5 μm in diameter or even smaller are found. PbWO$_4$ particles in turn are oval or rod shaped with the length up to the 2 μm and 0.5 μm in thickness. Particles size distribution of the PbWO$_4$ powder is more uniform than in the case of PbMoO$_4$. It was found, that the duration time of the synthesis used in the experiment has negligible or no influence on the morphology or particle size of the both powders. Although both materials adopt the same crystal system, they exhibit different morphologies. It may be concerned with the precursor of anions. In the case of PbMoO$_4$ the product precipitates immediately after mixing of reagents, whereas the PbWO$_4$ powder is obtained after the heat treatment. In this case the first step must be the hydrolysis of the metatungstate anion which is enhanced at the elevated temperature. Thereafter, when a sufficient amount of WO$_4^{2-}$ ions is produced, the solubility product will be exceeded and PbWO$_4$ precipitate. Such a two-step process could result in obtaining the different morphology for lead tungstate in comparison with lead molybdate. In addition, the pH of the reaction mixture may also play a role, namely at neutral pH, the hydrolysis of ammonium metatungstate should be enhanced, on the other hand Pb(OH)$_2$ may also precipitate due to the hydrolysis of lead acetate. For the PbWO$_4$ sample after 4 hours there are some round-shaped particles with a small hole in the middle of the particle. It may indicate, that at the elevated temperature also a dissolving process occurs. This effect was not observed in the case of lead molybdate probably due to the fact that PbWO$_4$ is more soluble salt than PbMoO$_4$.
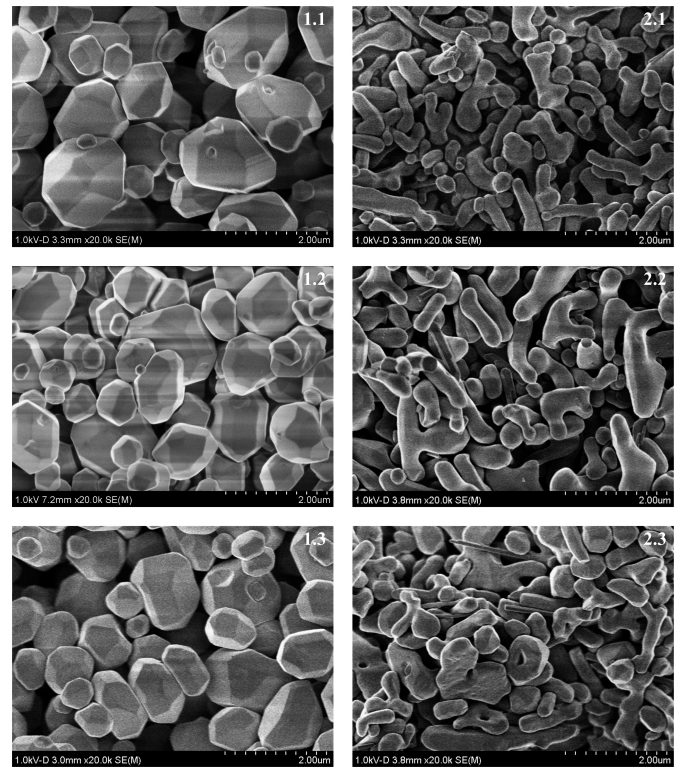
Diffuse reflectance spectroscopy is a simple and convenient method for the characterization of the powdery samples *i.e.* the determination of the value of the band gap E_g. The PbMoO$_4$ and PbWO$_4$ powders were grated in a mortar with BaSO$_4$ and the reflection spectra of such prepared samples were recorded. In order to obtain a reliable value of the band gap, the reflection spectra should be transformed into the absorption spectra. To this end, a Kubelka-Munk F^{KM} function was calculated as follows (Eq. 3):

$$F^{KM} = \frac{(1 - R(h\nu))^2}{2R(h\nu)} = \frac{\alpha(h\nu)}{S} \qquad (3)$$

where $R(h\nu)$ is the reflectance of the sample measured *vs.* BaSO$_4$ pellet (100% reflectivity standard). For the very small particles a scattering factor S is equal to 1 and the F^{KM} equals to the absorption coefficient α. The S factor may be regarded as a constant for bigger particles provided, that the thickness of the sample is much bigger than of individual particles [27]. Therefore, the dependence of F^{KM} on the wavelength can be treated as the absorption spectrum. In order to determine the E_g value from such a spectrum McLean analysis of the absorption edge was applied [28]. Since the indirect band gap was postulated for both PbMoO$_4$ and PbWO$_4$ crystals, the relation between the energy of an incident photon $h\nu$ and the F^{KM} along the absorption edge can be described as follows (Eq. 4):

$$\left(F^{KM} h\nu\right)^{1/2} = A\left(h\nu - E_g\right) \qquad (4)$$

where A is a constant.

Fig. 4 shows the diffuse reflectance spectrum (in the form of the Kubelka-Munk function) of the powdery sample of PbMoO$_4$ after 4 hours of synthesis. The value of the band gap determined for this sample equals to 3.20 eV $\pm$ 0.05 eV

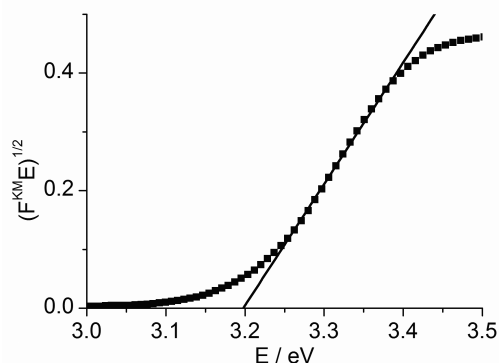and fits well the values reported in the literature (between 3.1 and 3.2 eV [2, 3]).

Fig. 4. The absorption spectrum of the PbMoO$_4$ sample after 4 hours of synthesis

The dependence of the band gap on the duration time of the synthesis for both lead molybdate and tungstate is shown in Fig. 5.
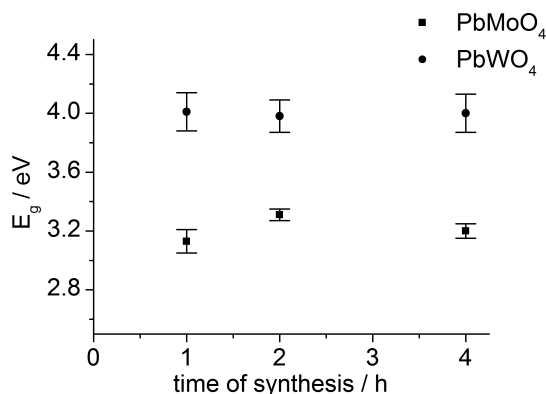

Fig. 5. The dependence of the band gap of the obtained samples on the time of the synthesis for both PbMoO$_4$ and PbWO$_4$

In the case of lead tungstate, the band gap does not depend on the duration time of the synthesis, the values oscillate around 4 eV. It well corresponds with the SEM images for this material, where the dimensions of the PbWO$_4$ particles are comparable. For the PbMoO$_4$ samples after 1 and 4 hours of the synthesis the value of the band gap is similar, whereas after 2 hours the band gap is wider. It could be concerned with some contribution of the small particles in the sample, however the morphology of the samples determined by the SEM is very similar. Error bars obtained for the PbWO$_4$ samples are almost two times bigger than for PbMoO$_4$, however they are still acceptable. This effect was caused by a dispersion of the smaller amount of lead tungstate in barium sulfate for the diffuse reflectance measurement in comparison with lead molybdate.

4. Conclusions

Both lead molybdate and tungstate in the form of micropowder were successfully synthesized using the microwave assisted hydrothermal route. It is environmentally friendly technique since no organic solvents are employed and no volatile products of the reaction are emitted. Moreover, dielectric heating is energy efficient process. This method enables obtaining phase pure highly crystalline materials. Adopted synthetic conditions led to obtaining both PbMoO$_4$ and PbWO$_4$ in the tetragonal crystal structure regardless of the duration time of the synthesis. The morphology of the samples also does not varies significantly with the time of the synthesis. The medium value of the band gap for lead molybdate equals to 3.2 eV whereas for lead tungstate it is higher and reaches 4.0 eV. Taking into account these values PbMoO$_4$ seems to be much more promising material for the photocatalytic applications, however for efficient harvesting of solar radiation it still needs a surface modification. On the other hand, surface modified lead tungstate could be also interesting material from the point of view of photocatalysis. For such purposes it is important, to obtain as high surface to volume ratio as possible without significant widening of the band gap.

Obtained materials require the further investigation in order to determine a flatband potential and photoelectrochemical properties. Thereafter it will be possible to evaluate its photocatalytic properties. It may also be possible to employ such materials for information processing.

REFERENCES

[1] Y. Z h a n g, N.A.W. H o l z w a r t h, R.T. W i l i a m s, Phys. Rev. B **57**, 12738 (1998).

[2] M. H a s h i m, C. H u, X. W a n g, X. L i, D. G u o, Appl. Surf. Sci. 258, (2012).

[3] M. S h e n, Q. Z h a n g, H. C h e n, T. P e n g, CrystEngComm **13**, 2785 (2011).

[4] A.W. S l e i g h t, Acta Crystallogr. B Struct. Sci. **28**, 2899 (1972).

[5] T. F u j i t a, I. K a w a d a, K. K a t o, Acta Crystallogr. B Struct. Sci. **33**, 162 (1977).

[6] M.W. S t o l t z f u s, P.M. W o o d w a r d, R. S e s h a d r i, J.-H. K l e p e i s, B. B u r s t e n, Inorg. Chem. 46, 3839 (2007).

[7] F.A. D a n e v i c h, B.V. G r i n y o v, S. H e n r y, M.B. K o s m y n a, H. K r a u s, N. K r u t y a k, V.M. K u d o v b e n k o, V.B. M i k h a i l i k, L.L. N a g o r n a y a, B.P. N a z a r e n k o, A.S. N i k o l a i k o, O.G. P o l i s c h u k, V.M. P u z i k o v, A.N. S h e k h o v t s o v, V.I. T r e t y a k, Y.Y. V o s t r e t s o v, Nucl. Instrum. Meth. A **622**, 608 (2010).

[8] H. K a d o w a k i, N. S a i t o, H. N i s h i y a m a, H. K o b a y a s h i, Y. S h i m o d a i r a, Y. I n o u e, J. Phys. Chem. C **111**, 439 (2007).

[9] H. F u, C. P a n, L. Z h a n g, Y. Z h u, Mat. Res. Bull. **42**, 696 (2007).

[10] P. L e c o q, I. D a f i n e i, E. A u f f r a y, M. S c h n e e g a n s, M.V. K o r z h i k, O.V. M i s s e v i t c h, V.B. P a v l e n k o, A.A. F e d o r o v, A.N. A n n e n k o v, V.L. K o s t y l e v d, V.D. L i g u n, Nucl. Instrum. Meth. A **365**, 291 (1995).

[11] E. Auffray, M. Korjik, A. Singovski, Experimental Study of Lead Tungstate Scintillator Proton-Induced Damage and Recovery, in: SCINT2011 11th International Conference on Inorganic Scintillators and their Applications, Giessen, 2011.

[12] G.M. Loiacono, J.F. Balascio, R. Bonner, A. Savage, J. Cryst. Growth **21**, 1 (1974).

[13] H.C. Zeng, J. Cryst. Growth **171**, 136 (1997).

[14] D. Piwowarska, S.M. Kaczmarek, M. Berkowski, J. Non-cryst. Solids **354**, 4437 (2008).

[15] K. Tanji, M. Ishii, Y. Usuki, M. Kobayashi, K. Hara, H. Takano, N. Senguttuvan, J. Cryst. Growth **204**, 505 (1999).

[16] R. Lacomba-Perales, J. Ruiz-Fuertes, D. Errandonea, D. Martinez-Garcia, A. Segura, EPL-Europhys. Lett. **83**, 37002-5 (2008).

[17] I. Vesselinov, J. Cryst. Growth **167**, 725 (1996).

[18] H.-L. Wang, X.-D. Ma, X.-F. Qian, J. Yin, Z.-K. Zhu, J. Solid State Chem. **177**, 4588 (2004).

[19] A. Phuruangrat, T. Thongtem, S. Thongtem, Curr. Appl Phys. **10**, 342 (2010).

[20] J. Geng, J.-J. Zhu, H.-Y. Chen, Cryst. Growth. Des. **6**, 321 (2006).

[21] A. Phuruangrat, T. Thongtem, S. Thongtem, J. Cryst. Growth **311**, 4076 (2009).

[22] P. Lidström, J. Tierney, B. Wathey, J. Westman, Tetrahedron **57**, 9225 (2001).

[23] C. Gabriel, S. Gabriel, E.H. Grant, B.S.J. Hastead, D.M.P. Mingos, Chem. Soc. Rev. **27**, 213 (1998).

[24] S. Galema, Chem. Soc. Rev. **26**, 233 (1997).

[25] V. Polshettiwar, R.S. Varma, Aqueous Microwave Assisted Chemistry: Synthesis and Catalysis, Cambridge 2012.

[26] E.E. Chao, K.L. Cheng, Talanta **24**, 247 (1977).

[27] M. Nowak, B. Kauch, P. Szperlich, Rev. Sci. Instrum. **80**, 461071 (2009).

[28] T.P. McLean, The absorption edge spectrum of semiconductors, in: A.F. Gibson (Ed.) Progress in Semiconductors, vol. 5, Heywood & Company Ltd., London, 1960.